Int. J. Electrochem. Sci., 8 **(2013)** 5108 - 5120

International Journal of
ELECTROCHEMICAL
SCIENCE
www.electrochemsci.org

Better Corrosion Management in Sodium Chloride Solution of Some Pieces Obtained from Metallurgical Iron Powder Ancorsteel 1000B Using Cadmium and Zinc Coatings to Protect Underlying Substrate

Adriana Samide[1,*], *Bogdan Tutunaru*[1], *Anca Didu*[1], *Catalin Luculescu*[2], *Cristian Tigae*[1], *Cezar Spînu*[1], *and Mircea Preda*[1]

[1]University of Craiova, Faculty of Sciences, Department of Chemistry, Calea Bucuresti 107i, Craiova, Romania
[2]INFLPR-Bucharest, Laser Department, Atomistilor 409, 077125 Magurele, Romania
[*]E-mail: samide_adriana@yahoo.com

Received: 15 February 2013 / *Accepted:* 7 March 2013 / *Published:* 1 April 2013

The iron powder Ancorsteel 1000B was used to manufacture some pieces (IPAS), by pressing at 400 MPa, followed by sintering at 1150 ^{o}C. In order to improve their corrosion resistance in 1.0 % NaCl solution, certain specimens were submitted to protection with cadmium and zinc coatings. The corrosion behaviour of unprotected and protected IPAS samples was discussed according to electrochemical measurements such as: potentiodynamic polarization and electrochemical impedance spectroscopy (EIS), in association with Scanning Electron Microscopy and Energy Dispersive X-ray Spectroscopy (SEM/EDS) technique. Electrochemical measurements demonstrated the barrier properties of cadmium coating and the sacrificial protection of zinc deposit. SEM/EDS showed the same trend, meaning that the cadmium coating is more persistent, after corrosion, than zinc deposit.

Keywords: metallurgical iron powder; protection; corrosion; electrochemical measurements; SEM/EDS technique.

1. INTRODUCTION

Porous materials prepared by powder metallurgy offer many advantages and are widely used in airplanes, trains and automobiles. In the powder metallurgy technique, this type of materials, which are mainly Fe, Cu and Al based, are prepared by pressing and sintering metal powders with the addition of lubricants and friction particles [1-3]. The main attraction of powder metallurgy is its ability to manufacture metallic components with high friction coefficients, good heat resistance, no metal loses

in machining, high quality and low costs. However, wrought materials have lower corrosion rates and better mechanical properties, so the use of metallurgical materials are often limited [4].

Knowing that porosity influences the mechanisms of processes that occur on the surface of metallurgical materials, composition, compaction pressure, powder size, pore size and shape, it has an important influence on the microstructure and hardness [5, 6]. Low porosity was always associated with high compaction pressure and larger powder size. Smaller powder size and high compaction pressure lead to higher hardness. The processing parameters affect surface topography, and as a consequence, the mechanical properties and corrosion resistance in different aggressive environments [7]. Cooling method applied after sintering, also influences the corrosion properties. Duplex stainless steel produced by powder metallurgy has different corrosion rates, in 1 M NaCl solution, corresponding to different rates of cooling [8]. Sintering temperature is another parameter that influences electrochemical behaviour of steels manufactured by powder metallurgy. 316L and 434L stainless steels sintered at higher temperature present better corrosion resistance, while austenitic SS were superior to feritic SS [9]. Linear polarization resistance and electrochemical noise techniques were used to determine the corrosion behaviour of AISI 409Nb with and without addition of boron after immersion in 0.5 M H_2SO_4 and 0.5 M NaCl [10]. Low pH, high concentrations of chloride, and organic matter changes the corrosion potential of packed iron powder electrode lead to breakdown of passive film [11]. Particle size, packing density and purity of the powders are important factors for ferrate generation at iron powder electrodes. The surface of iron electrode after electrolysis in 14 M NaOH was analyzed by X-ray diffraction and X-ray photoelectron spectroscopy [12].

Due to the need for improved performance of metallurgical powder, different methods can be used: adding alloying elements or compounds, pre-alloying, premixing, passivation or pre-passivation. Electrochemical behaviour of powder metallurgical 316L alloy was improved by prepassivation in 20% nitric acid; corrosion resistance was studied using open circuit potentiometry, linear polarization and zero resistance ammeter techniques [13]. Iron powder micro particles were coated with a poly (methyl methacrylate) (PMMA) film by electro polymerization in a fluidized bed reactor [14].

Plating of metallic powder particles by polymeric coating modifies surface properties of materials used in powder metallurgy. Electrochemical coating of powder materials may be efficiently realized. Ni and Ni-Co were electrodeposited onto Fe powder from a sulphate electrolyte. Metallic coatings were analyzed by scanning electron microscope and optical microscope. Voltametric measurements in 0.5 M H_2SO_4 and 3% NaCl indicate an improvement of corrosion resistance [15]. Electrodeposition of cadmium and zinc onto different substrates is widely used in production of electronic materials for conductive devices [16-20]. Recent articles have reported the electrodeposition of Cd(S/Se/Te), Zn(S/Se/Te) binary alloys and CdZn(S/Se/Te) ternary with applications in infra-red (IR), X-ray and gamma radiation detections and in solar cell panels [21, 22].

This research reports the corrosion behaviour in 1.0 % NaCl solution, of some unprotected and protected IPAS samples with cadmium and zinc coatings using electrochemical measurements and SEM/EDS technique. In order to discuss the sacrificial properties of Zn coating in comparison with barrier properties of cadmium deposit the work was structured as follows: the itinerary of technology to manufacture of pieces is presented in “Materials and Methods” section; in the first part of “Results and Discussion” section the SEM/EDS for unprotected and protected IPAS samples, before corrosion

is described; corrosion tests are revealed by electrochemical results, which are discussed for reference IPAS compared with the protected surfaces with cadmium and zinc deposits; these are followed by comments and conclusions about the coatings resistance in 1.0 % NaCl, showing SEM/EDS results after corrosion processes occurrence due to this environment.

2. MATERIALS AND METHODS

2.1. Technological itinerary of compacts (IPAS) manufacture

Metallurgical iron powder, Höeganaes Ancorsteel 1000B with an apparent density of 2.92 g/cm^3, (its particles size between 100 μm -125 μm) was used for compaction at 400 MPa, in order to obtain cylindrical compacts which were submitted to corrosion tests. In Figure 1 is shown SEM/EDS analysis of this powder related to its appearance and composition.

The technological itinerary to obtain cylindrical compacts includes the following steps: (i) the achievement of cylindrical compacts; (ii) the sintering of achieved parts [23].

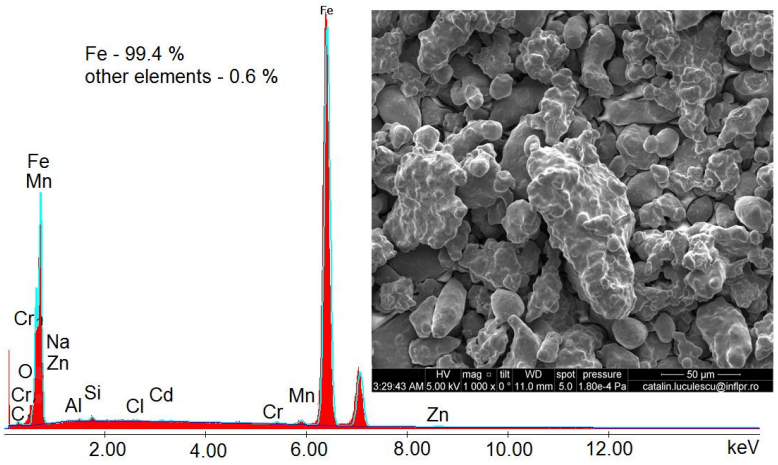

Figure 1. SEM image and EDS spectrum of metallurgical iron powder, Ancorsteel 1000B.

The achievement of these compacts consists in mixing of iron powder Ancorsteel 1000B with 1% zinc stearate, followed by homogenization, and the compaction within a proper matrix to a pressure of 400 MPa using a press, OMCN 100 Tons type. The obtained specimens were sintered in an oven with controlled atmosphere (argon), in order to avoid the oxidation and carburization of the surfaces, at a temperature of 1150 °C, using a L1207 / 220 WEB laboratory furnace. Thus, after sintering, compacts with a density of 6.6 g/cm^3 and minor contractions that reduced their sizes with approx. 0.3% were obtained. Cylindrical samples (IPAS) have the diameter (φ = 20 mm), much larger than their height (1.8-2mm). Dimensions and aspect can be seen in Figure 2.

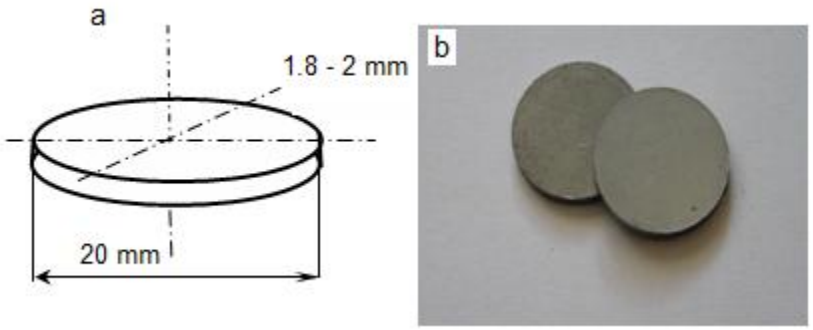

Figure 2. Dimensions (a) and visual appearance (b) of sample (IPAS) obtained by pressing at 400 MPa and sintering at 1150 °C.

2.2. Surface protection of IPAS by metals electrodeposition

The compacts obtained by pressing at 400 MPa and sintering at 1150 °C, were coated with zinc and cadmium deposits, in order to protect their surfaces against corrosion in 1.0 % NaCl solution. Before electrodeposition, the specimens were successively polished with 200, 600, 800 grades of sandpaper, ultrasonically cleaned with bi-distilled water, degreased with acetone, and then stored in a vacuum desiccator. For both metal deposits numerous compositions for plating baths have been used, but because of parts porosity improperly deposits were obtained.

The satisfactory results were obtained from cyanide baths. Thus, zinc baths consisted of the following composition: 90 g/L zinc cyanide, 125 g/L sodium cyanide and 120 g/L sodium hydroxide. A current density of 4 A/dm^3, at temperature of 28 °C for 30 minutes, was applied. Cadmium deposits were obtained from plating baths containing: 20 g/L cadmium oxide, 110g/L sodium cyanide, 7.5 g/L sodium hydroxide, operating parameters being: current density of 2 A/dm^3; temperature of 28 °C; electrodeposition time of 20 minutes.

2.3. Corrosion tests

The corrosion resistance of IPAS, both unprotected as well as protected with Zn and Cd deposits, has been investigated using electrochemical methods such as: potentiodynamic polarization and electrochemical impedance spectroscopy (EIS) in association with Scanning Electron Microscopy with Energy Dispersive X-ray Spectroscopy (SEM/EDS) technique.

2.3.1. Electrochemical measurements

Electrochemical measurements were performed using an electrochemical system, VoltaLab 40, with a personal computer and VoltaMaster 4 software. A standard corrosion cell with three electrodes was used: a working electrode made of tested material (IPAS unprotected and protected with Zn and Cd coatings) with an active surface of 1.57 cm^2; an auxiliary platinum plate electrode (area of 1.0 cm^2); a reference electrode of Ag/AgCl$_{sat}$. The immersion time of the plates in 1.0 % NaCl was of 20

minutes in open circuit, at room temperature. Potentiodynamic polarization curves were obtained with the scan rate of 1.0 mV/s.

Electrochemical impedance spectroscopy (EIS) was measured in a frequency range from 10^5 Hz to 10^{-1} Hz by a parturition signal of 10 mV amplitude peak to peak at room temperature, after the immersion time of 20 minutes in open circuit. All reagents were obtained from Fluka.

2.3.2. SEM/EDS technique

The surfaces' morphology was inspected by scanning electron microscopy (SEM), in a FEI Inspect S microscope. Energy-dispersive X-ray spectroscopy (EDS) was performed using a SiLi based energy-dispersive detector from EDAX Inc.

3. RESULTS AND DISCUSSION

3.1. Surface characterization of unprotected and protected IPAS sample before corrosion

In Figure 3 the SEM images and EDS spectra of IPAS sample unprotected (a) and protected with Cd (b) and Zn (c) coatings are shown before corrosion processes occurrence. Surface morphology of reference IPAS sample (Fig.3a) obtained at 400 MPa compacting pressure, a relative uniformity, showing characteristic grains and porosity is evidenced. EDS spectrum (Fig.3a) indicates the iron in high proportion and other elements, as similar impurities, like those presented in iron powder (Fig.1). The concentration of other elements is higher compared to iron powder, probably because the compaction produces their zonal clustering. The increase of carbon content is due to the presence of zinc stearate, as lubricant in the process of parts manufacture.

Also, due to sintering in inert atmosphere, oxygen is in a small amount, below the detection limit. SEM images from Figures 3b and 3c show the characteristic morphologies of cadmium (b) and zinc (c) coatings electrodeposited on IPAS surface. It is difficult to assess these morphologies would be characteristic of a metal or its oxide. More probably, the feature of metallic nucleation, forming a matrix in which are embedded certain oxide molecules, is relatively nuanced.

On the other hand, the oxygen proportion can be due to an adsorption process from plating baths during electrodeposition, and/or specific oxides formation (spectra from Figs.3b and c). In both cases, the metal proportion has the highest value, indicating that a characteristic layer on IPAS surface was electrodeposed. Iron proportion is very small (spectra from Figs.3b and 3c), suggesting an effective electrodeposition, with formation of protective layer that improve the uniformity of IPAS surfaces, and consequently, the granules are not so emphasized. Other elements, which are given in mentioned spectra, are due to exposure of samples in the electrolytes from the plating baths.

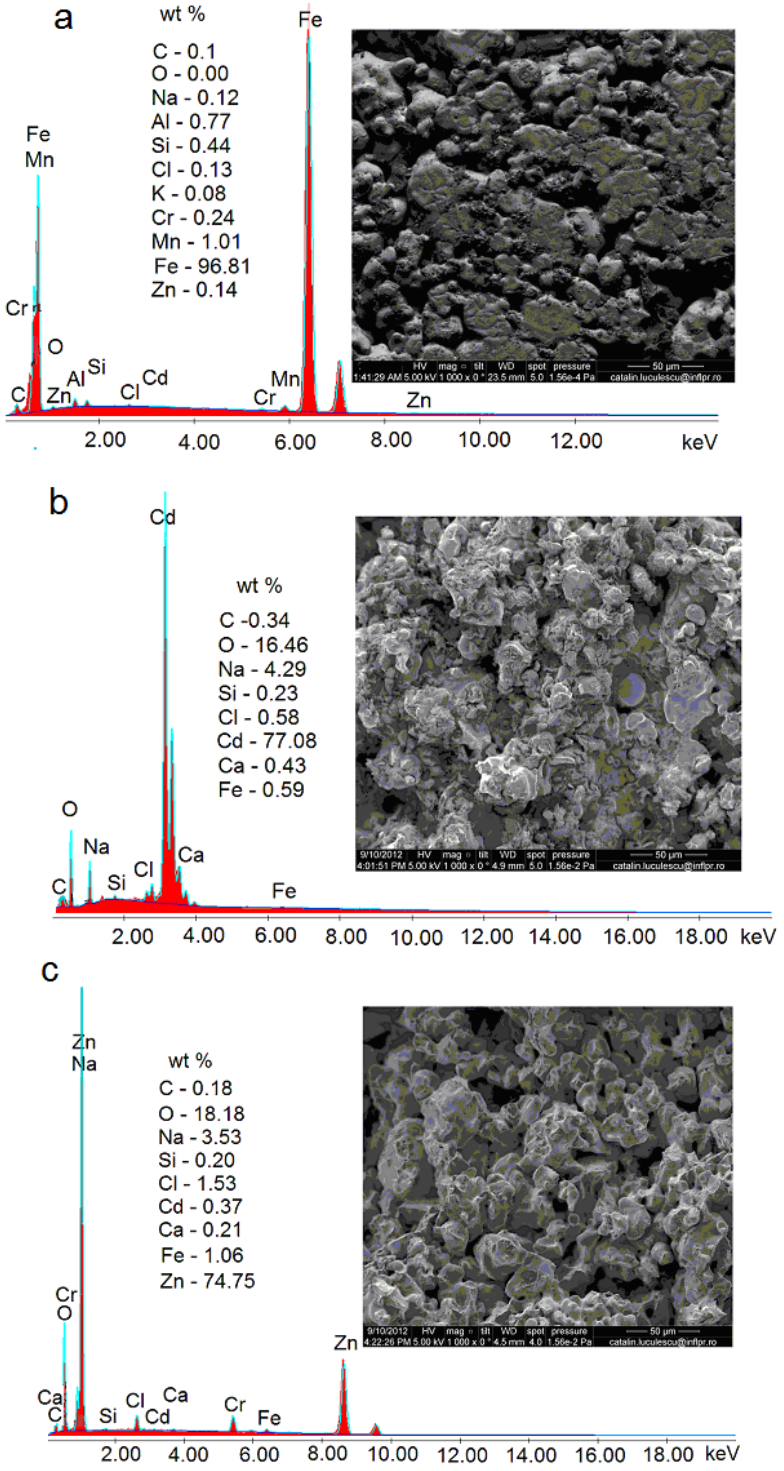

Figure 3. SEM images and EDS spectra of IPAS before corrosion: a – reference sample; b – protected specimen with cadmium coating; c – protected specimen with zinc coating.

3.2. Corrosion tests

Both the samples unprotected, as well as protected with cadmium and zinc deposits were exposed to corrosion in 1.0 % NaCl solution, at room temperature. The corrosion tests were discussed

according to the results obtained from electrochemical measurements associated with SEM/EDS analysis.

3.2.1. Electrochemical measurements

In Figure 4 the results of electrochemical measurements are shown, relating the potentiodynamic polarization (Fig.4a) and impedance spectroscopy given as Nyquist graph (Fig.4b) and Bode diagrams (Figs. 4c and 4d).

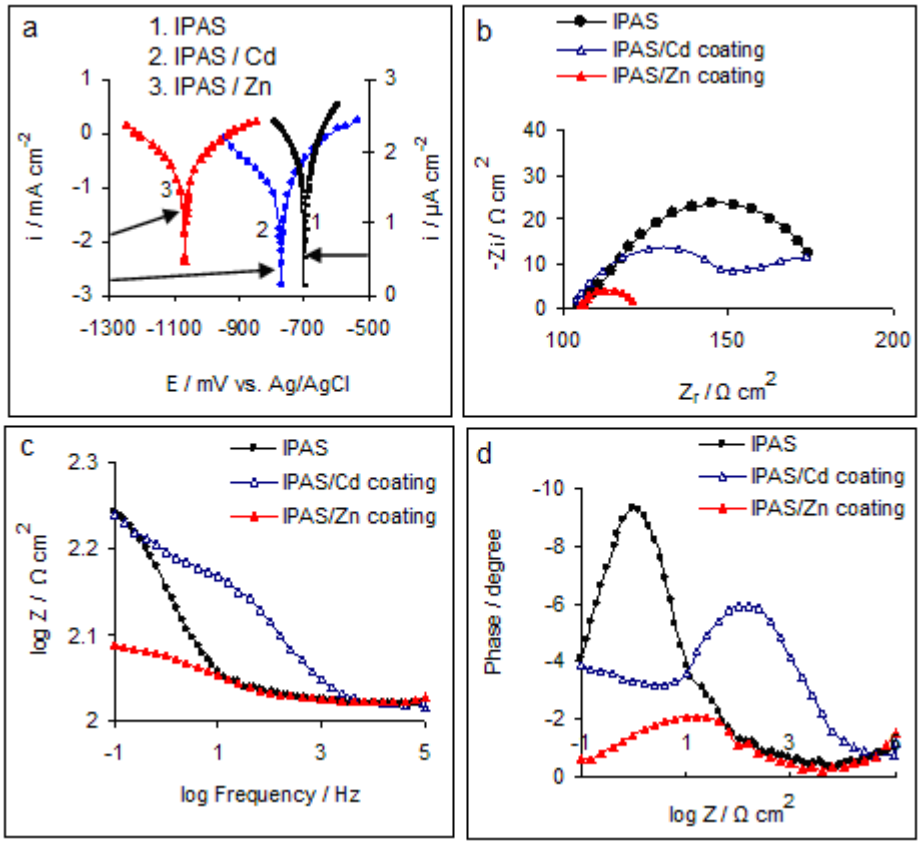

Figure 4. The results of electrochemical measurements for unprotected and protected IPAS samples corroded in 1.0 % NaCl solution, at room temperature: a - potentiodynamic curves; b - Nyquist Diagram; c - impedance Bode diagram; d - phase Bode diagram

Cadmium and zinc coatings used as surfaces finishes provide adequate protection against corrosion for many substrates, in various aggressive environments, having the performance feature that include corrosion sacrificially to substrate, stability of corrosion by products, coating adherence and low dissolution rates in corrosive media [24, 25].

Because the coating must be sacrificial in relation to its substrate, the positioning of protective layer in relation to the substrate in the corrosion potential (E_{corr}) scale in a corrosive medium is important [26]. The corrosion potential (E_{corr}) measured indicates the tendency of cadmium and zinc, respectively, to corrode in 1.0 % NaCl solution. By comparing the corrosion potential (E_{corr}) of two

coatings (Fig.4a), it is possible to conclude which was intensely corroded. In case of zinc, the dissolution rate is high due to the large corrosion potential difference between the underlying substrate (IPAS) and the zinc coating (Table 1). Cadmium possesses good barrier properties, being less susceptible to corrosion in 1.0 % NaCl solution, its corrosion potential (E_{corr}) being much closer to IPAS substrate E_{corr} (Table 1), than that measured for zinc coating.

To evaluate the barrier properties of cadmium and zinc coatings to diminish the corrosion of IPAS substrate in 1.0 % NaCl solution, potentiodynamic studies were performed in order to calculate the corrosion current (i_{corr}) by extrapolation anodic and cathodic Tafel lines to corrosion potential (E_{corr}). The i_{corr} observed for zinc coating is higher than that obtained for cadmium (Table 1). Since the corrosion rate is directly proportional to the corrosion current (i_{corr}), the trend remained the same with cadmium having the lowest corrosion rate in 1.0 % NaCl solution (Table 1).

Table1. Electrochemical parameters obtained from potentiodynamic polarization for IPAS sample corroded in 1.0 % NaCl solution, at room temperature.

Sample	E_{corr} / mV vs. $Ag/AgCl_{sat}$	i_{corr} / $\mu A\ cm^{-2}$	b_a / $mV\ dec^{-1}$	b_c / $mV\ dec^{-1}$
IPAS	-701	225	269	172
IPAS/Cd coating	-770	119	226	157
IPAS/Zn coating	-1069	214	261	152

From Table 1, it can be seen that cadmium has the lowest corrosion current, while zinc coating corrodes with a similar rate to that the substrate, suggesting that zinc layer had provided less efficient barrier protection. On the other hand, anodic Tafel slope suggests the value of cathodic polarization, which is necessary to diminish the corrosion rate, meaning that, to reduce the corrosion with a given value, anodic Tafel slope must considerably increase with the displacement of polarization in the negative direction [27].

The results show that, anodic Tafel slope values of uncovered IPAS sample and the zinc layer have reached very close values, although there are significant differences of polarization, which could explain the similarity between corrosion current values, obtained in both cases above mentioned. Based on these data we may conclude that the sacrificial properties of zinc coating offer some level of sacrificial protection to the underlying IPAS substrate, meaning that this coating has a short life due to its corrosion rate, but multiple layers of zinc could be beneficial to cover this material to control its corrosion. The potential of zinc was stable at -1069 mV vs. Ag/AgClsat, while the corrosion potential of cadmium coating was more positive (-770 mV vs. Ag/AgCl), consequently the polarization curve of cadmium was shifted in positive direction of potentials, with respect to zinc, which in its turn, decreases the corrosion current value from 214 $\mu A\ cm^{-2}$ to 119 $\mu A\ cm^{-2}$. Therefore, zinc protects the IPAS surface acting as sacrificial anode, while cadmium forms an effective barrier at the interface of substrate/electrolyte, which significantly decreases the corrosion current of IPAS.

The EIS measurements (Figs.4b, 4c and 4d) confirm the results obtained from potentiodynamic polarization. The Nyguist impedance diagram obtained in 1 % NaCl solution presented in Figure 4b, shows a well defined capacitive loops for IPAS sample and zinc coating, and there was no evidence of other inductive or capacitive loops at lower frequencies. The corrosion in both cases is purely charge transfer controlled, as revealed from the semicircles shape of Nyquist spectrum [28, 29], but a retardation effects on zinc coating loop is observed, indicating that this is primordially dissolved in relation with its underlying substrate (IPAS). It is known that, the protective properties of the coatings increase with increasing diameter of the semicircle [28, 30, 31], consequently cadmium coating provides better protection than that zinc coating offered. Also, cadmium capacitive loop decreased in relation with that of its underlying substrate (IPAS), and finally arrives at a line, in the low frequencies region. Moreover, in high frequencies region, the semicircle diameter obtained for cadmium is greater than that of zinc coating, indicating that, cadmium provides better protection for IPAS surface compared with zinc. The observed retardation effect on cadmium coating in relation with that of its underlying substrate (IPAS) could be explained by a strong geometrical blocking [32] which takes place on the restricted area of active sites of IPAS surface, knowing the fact that, surface treatments may affect the electrochemical activity of the electrodes [32, 33]. Figures 4c and 4d present the Bode plots resulted from the EIS measurements, in which a comparison between unprotected and protected IPAS samples is shown. From Figure 4c, it can be seen that the impedance response of IPAS sample in 1.0 % NaCl solution shows significantly change for IPAS coated with cadmium, indicating that the impedance values reach higher levels than those of unprotected sample, and consequently its protection efficiency increases. These changes are more significant in the frequency range of 10^4-1.0 Hz. The first remark may refer to the fact that the cadmium coating acts as a barrier against corrosion of its underlying substrate (IPAS). From Figure 4c it can be predicted the sacrificial properties of zinc coating, by means of its impedance responses, which reach the lowest levels, compared to both IPAS samples, uncoated and coated with cadmium. The same conclusions can be remarked from Bode diagram (Fig.4d). In the corresponding impedance profiles in the Bode format, one phase angle maximum is discernible (Fig.4d), which is induced by double layer capacitance at high frequencies [34]. Bode graph for cadmium coating differ from those obtained for IPAS and zinc coating, by displaying its wave, consequently the phase angle maximum, in higher frequencies region, versus position waves corresponding IPAS and zinc coating respectively. We assume that, the polarization resistance cannot be considered a factor that indicates corrosion resistance of the underlying IPAS, if the substrate is protected and more so, if it forms salt film which may be promoted from NaCl solution [35].

3.2.2. SEM/EDS results after corrosion tests

In Figure 5 there are presented SEM images and EDS spectra of IPAS specimens after potentiodynamic measurements. The results will be commented in comparison with those were obtained before corrosion. The main difference between IPAS uncorroded reference sample (Fig.3a) and unprotected substrate corroded in 1.0 % NaCl solution (Fig.5a), consists in a considerable

increase of oxygen peak height, meaning that, the corrosion products of iron may be evidenced and the adsorbed oxygen can be noted. Many researchers used in their studies different techniques such as: XPS, SEM/EDS, Mössbauer spectroscopy to detect the corrosion products of iron [36-42]. Thus, these studies reported that at pH around of 5 value, the main corrosion product consists in Fe^{3+} species resembling those shown by amorphous Fe^{3+} oxyhydroxides: anhydrous and/or hydrated FeO(OH) such as iron (III) hydroxide and ferrihydrite in mixture with Fe_2O_3 and Fe_3O_4 [36-42].

On the other hand, the SEM image, from Fig.5a, shows a different morphology than that was presented in Fig.3a, confirming an uneven layer formation on IPAS surface, which affects a large area, by appearance of some cavities. These could become, in time, much deeper, causing in depth cracking of parts. These shortcomings were removed by cadmium plating, as shown Figure 5b.

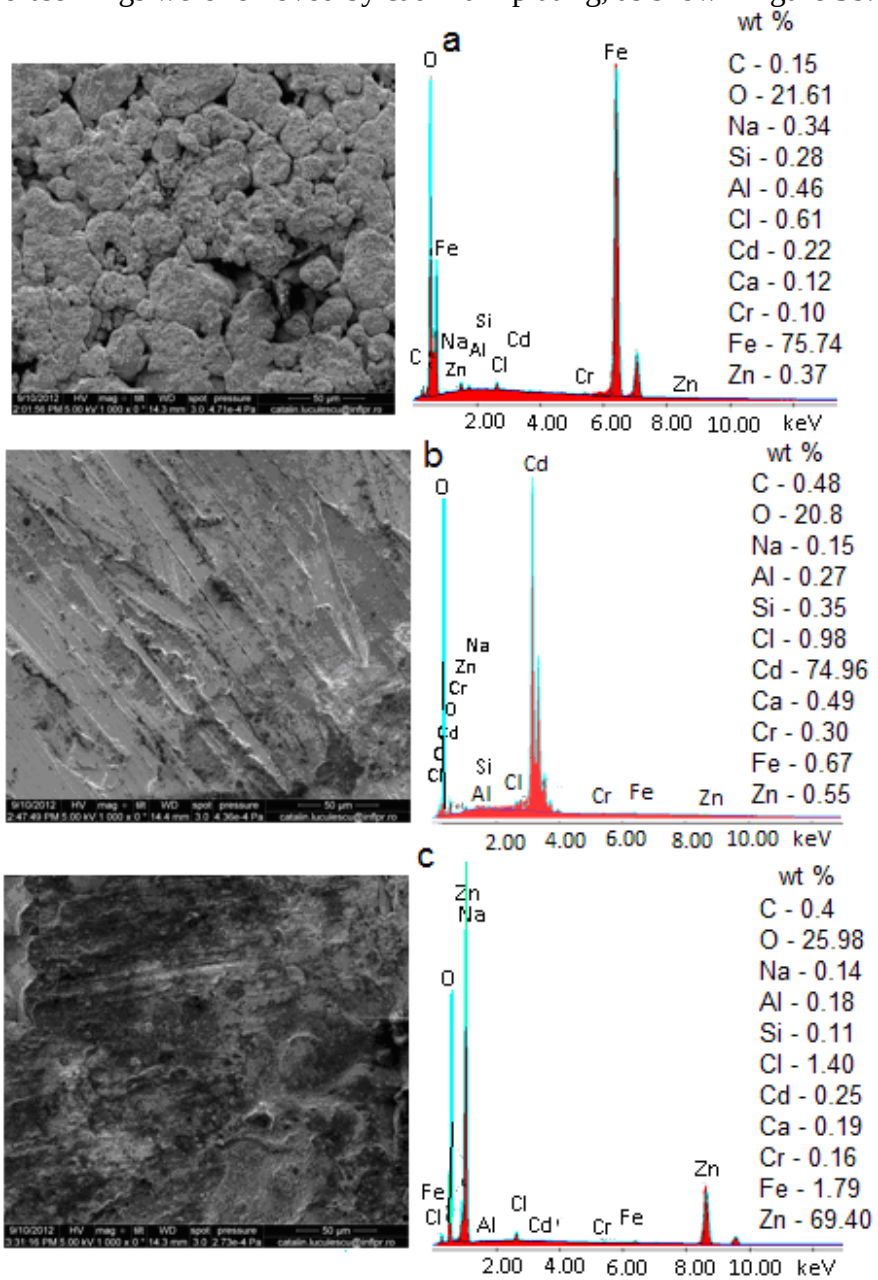

Figure 5. SEM images and EDS spectra of IPAS after corrosion processes occurrence: a – reference sample; b – protected specimen with cadmium coating; c – protected specimen with zinc coating.

SEM image from Figure 5b shows a relatively smooth surface, that is attributed to a cadmium coating, that was enough resistant to corrosion processes. Moreover, the IPAS characteristic granules are not observable, and their surface is relatively uniform and completely covered with cadmium layer. By inspection the EDS spectrum, from Figure 5b, it can be concluded that the cadmium proportion has decreased with 3 % compared with that found before corrosion (Fig.3b), indicating that, the cadmium coating was very resistant in 1.0 % NaCl solution, and it may act as a barrier against corrosion for its underlying substrate IPAS.

Other elements observed in Figure 5b come from plating bath, being known that Cd^{2+} readily forms complexes with cyanide, such as: $[Cd(CN)_4]^{2-}$ and $[Cd(CN)_6]^{4-}$ and/or hydroxocadmiates, for example, $Na_2[Cd(OH)_4]$. Moreover, iron proportion is very small, confirming that the cadmium coating was not affected, after corrosion process occurrence, being stable, and its adherence to underlying substrate (IPAS) is strong. Unlike cadmium, zinc coating was damaged by corrosion, and it has become thinner on some parts of the surface, as can be seen in Figure 5c, due to its higher corrosion rate than that of cadmium. In the initial stage of zinc corrosion, its oxide instantaneously occurs [43], but at the same time it must be considered that, in the presence of chloride ions, zinc hydrochlorides such as, $Zn_5(OH)_8Cl_2$ could be formed [43]. The iron proportion could be attributed to both underlying substrate (IPAS) as well as some iron corrosion products, which would form in a small amount, because zinc layer acts as a sacrificial anode, its barrier properties being less obvious than those of cadmium coating.

4. CONCLUSIONS

Metallurgical powder, Ancorsteel 1000B, was subjected to pressing process at 400 MPa, followed by sintering at 1150 ^{o}C, in order to get some pieces (IPAS) with good corrosion properties.

Particular samples were submitted to zinc and cadmium plating, to achieve a smoother surface than that of unprotected sample, and to protect them, in order to perform a good corrosion management in 1.0 % NaCl solution.

The corrosion behaviour of unprotected and protected IPAS samples was discussed according to the electrochemical measurements and SEM/EDS technique. The corrosion current obtained from potentiodynamic polarization has the lowest value for covered IPAS sample with cadmium coating, showing its effective barrier properties. On the other hand, zinc coating was dissolved with the highest rate, being a sacrificial anode in relation with its underlying substrate IPAS, thus, offering some level of sacrificial protection. EIS confirms that the trend remained the same with cadmium, having a better corrosion resistance than of zinc coating in 1.0 % NaCl solution.

SEM images confirm that protected layers have remained, after developing of corrosion processes. Moreover, a significant change of surface morphology of unprotected sample, after corrosion, was highlighted. EDS spectra are in full compliance with the above mentioned, in that, they confirm the formation of iron corrosion products on the unprotected sample surface, and that the protective layers persist after corrosion, these being attributed to metallic phase of zinc or cadmium, and/or to oxides, or other their corrosion compounds.

ACKNOWLEDGEMENTS

This study was partially supported by POSDRU/88/1.5/S/49516, Project ID 59516 (2009), co-financed by the European Social Fund – Investing in People, within the Sectorial Operational Programme Human Resources Development 2007-2013.

References

1. H. Ashassi-Sorkhabi, D. Seifzadeh and H. Harrafi, *J. Iran. Chem. Soc.*, 4 (2007) 72.
2. J. Li, Y. Yin and H. Ma, *Tribology Int.*, 38 (2005) 159.
3. R.Z. Xu, Powder Metallurgy Structural Materials, Changsha Publishing Company of Central South University of Technology, 2002.
4. A. Bautista, F. Velasco, S. Guzman, D. de la Fuente, F. Cayuela and M. Morcillo, *Rev. Metal Madrid*, 42 (2006) 175.
5. J. D. B. de Mello, A. Klein, R. Binder and I.M. Hutchings, *Powder Metallurgy*, 44 (2001) 1.
6. Yashwant Mehta, Shefali Trivedi, K. Chandra and P. S. Mishra, *Sadhana*, 35 (2010) 469.
7. J.D.B. de Mello, *Materials Res.*, 8 (2005) 135.
8. L.A. Dobrzanski, Z. Brytan, M. Actis Grande and M. Rosso, *Journal of Achievements in Materials and Manufacturing Engineering*, 19 (2006) 38.
9. J. Shankar, A. Upadhyaya and R. Balasubramaniam, *Corros. Sci.*, 46 (2004) 487.
10. J.A. Cabral-Miramontes, J.D. Barceinas-Sánchez, C.A. Poblano-Salas, G.K. Pedraza-Basulto, D. Nieves-Mendoza, P.C. Zambrano-Robledo, F. Almeraya-Calderón and J.G. Chacón-Nava, *Int. J. Electrochem. Sci.*, 8 (2013) 564.
11. J.T. Nurmi and P.G. Tratnyek, *Corros. Sci.*, 50 (2008) 144.
12. M. de Koninck, T. Brousse and D. Belanger, *Electrochim. Acta*, 48 (2003) 1425.
13. B. Shahabi Kargar, M.H. Moayed, A. Babakhani and A. Davoodi, *Corros. Sci.*, 53 (2011) 135.
14. A. Orinak, R. Orinakova, A. Heile, I. Talian, M. Terhorst and H.F. Arlinghaus, *Surf. Sci.*, 601 (2007) 4158.
15. Z. Feckova, *Journal of Metals, Materials and Minerals*, 17 (2007) 41.
16. A. Dolati, A. Afshar and H. Ghasemi, *Mater. Chem. Phys.*, 94 (2005) 23.
17. S. Maupai, Y. Zhang and P. Schmuki, *Surf. Sci.*, 527 (2003) L165.
18. F. Kadirgan, D. Mao, W. Song, T. Ohno and B. McCandless, *Turk. J. Chem.*, 24 (2000) 21.
19. C.K. Sarangi, B.C. Tripathy, I.N. Bhattacharya, T. Subbaiah, S.C. Das and B.K. Mishra, *Miner. Eng.*, 22 (2009) 1266.
20. A. Biswal, K. Padhy, C.K. Sarangi, B.C. Tripathy, I.N. Bhattacharya and T. Subbaiah, *Hydrometallurgy*, 117-118 (2012) 13.
21. F. Loglio, M. Innocenti, G. Pezzatini and M.L. Foresti, *J. Electroanal. Chem.*, 562 (2004) 117.
22. T. Gandhi, K.S. Raja and M. Misra, *Electrochim. Acta*, 51 (2006) 5932.
23. C. Amsallem, A. Gaucher and G. Guillot, *Wear*, 23 (1973) 97.
24. R. Mason, M. Neidbalson and M. Klingenberg, *Metal Finishing*, 108 (2010) 12.
25. T. Murai, *Metal Finishing*, 107 (2009) 41.
26. M. Gavrila, J. P. Millet, H. Mazille, D. Marchandise and J. M. Cuntz, *Surf. Coat. Tech.*, 123 (2000) 164.
27. T. Badea, G. E. Ciura and A. Cojocaru, *Corrosion and its Control. Electrochemical Fundaments*, Matrix Rom Ed., Bucharest, (2000) p. 231.
28. R. Sekar, C. Eagammai and S. Jayakrishnan, *J. Appl. Electrochem.*, 40 (2010) 49.
29. F. Mansfield, W. Kendig and S. Tasi, *Corros.*, 38 (1982) 570.
30. S. Survilline, A. Cesuniene and R. Juskena, *Trans. Inst. Met. Finish.*, 82 (2004) 18.
31. S. Survilline, V. Jasualaitiene and A. Cesuniene, *Trans. Inst. Met. Finish.*, 83 (2005) 130.
32. D. Becker and K. Jüttner, *J. Appl. Electrochem.*, 33 (2003) 959.

33. F. Marken, C.A. Paddon and D. Asogan, *Electrochem. Commun.*, 4 (2002) 62.
34. R. Solmas, G. Kardas, B. Yazicl and M. Erbil, *Colloids and Surfaces A: Physicochem. Eng. Aspects*, 312 (2008) 7.
35. *Corrosion* Studies - Shodhganga, http://shodhganga.inflibnet.ac.in/bitstream/10603/1844/12/12_chapter%205.pdf
36. X. Fan, X. Guan, J. Ma and H. Ai, *J. Environ. Sci.*, 21 (2009) 1028.
37. A. Samide and B. Tutunaru, *J. Environ. Sci. Healt. A*, 46 (2011) 1713.
38. A. Moanta, A. Samide, C. Ionescu, B. Tutunaru, A. Dobritescu, A. Fruchier and V. Barragan-Montero, *Int. J. Electrochem. Sci.*, 8 (2013) 780.
39. A. Samide, I. Bibicu, M.S. Rogalski and M. Preda, *Corros. Sci.*, 47 (2005) 1119.
40. A. Samide and I. Bibicu, *Surf. Interface Anal.*, 40 (2008) 944.
41. A. Samide, I. Bibicu, M. Agiu and M. Preda, *Mater. Lett.*, 62 (2008) 320.
42. A. Samide, I. Bibicu and E. Turcanu, *Chem. Eng. Commun.*, 196 (2009) 1008.
43. O. Girčienë, L. Gudavičiutë, R. Juskenas and R. Ramanauska, S*urf. Coat. Techn.*, 203 (2009), 3072.